

Vertical profiles of biospheric and fossil fuel-derived CO₂ and fossil fuel CO₂ : CO ratios from airborne measurements of $\Delta^{14}\text{C}$, CO₂ and CO above Colorado, USA

By HEATHER D. GRAVEN^{1*}†, BRITTON B. STEPHENS², THOMAS P. GUILDERSON^{3,4}, TERESA L. CAMPOS², DAVID S. SCHIMEL⁵, J. ELLIOTT CAMPBELL⁶ and RALPH F. KEELING¹, ¹*Scripps Institution of Oceanography, University of California - San Diego, La Jolla, California, USA*; ²*National Center for Atmospheric Research, Boulder, Colorado, USA*; ³*Center for Accelerator Mass Spectrometry, Lawrence Livermore National Laboratory, Livermore, California, USA*; ⁴*Department of Ocean Sciences, University of California - Santa Cruz, Santa Cruz, California, USA*; ⁵*National Ecological Observatory Network, Boulder, Colorado, USA*; ⁶*College of Engineering, University of California-Merced, Merced, California, USA*

(Manuscript received 22 August 2008; in final form 3 March 2009)

ABSTRACT

Measurements of $\Delta^{14}\text{C}$ in atmospheric CO₂ are an effective method of separating CO₂ additions from fossil fuel and biospheric sources or sinks of CO₂. We illustrate this technique with vertical profiles of CO₂ and $\Delta^{14}\text{C}$ analysed in whole air flask samples collected above Colorado, USA in May and July 2004. Comparison of lower tropospheric composition to cleaner air at higher altitudes (>5 km) revealed considerable additions from respiration in the morning in both urban and rural locations. Afternoon concentrations were mainly governed by fossil fuel emissions and boundary layer depth, also showing net biospheric CO₂ uptake in some cases. We estimate local industrial CO₂:CO emission ratios using in situ measurements of CO concentration. Ratios are found to vary by 100% and average 57 mole CO₂:1 mole CO, higher than expected from emissions inventories. Uncertainty in CO₂ from different sources was ± 1.1 to ± 4.1 ppm for addition or uptake of -4.6 to 55.8 ppm, limited by $\Delta^{14}\text{C}$ measurement precision and uncertainty in background $\Delta^{14}\text{C}$ and CO₂ levels.

1. Introduction

Observations of atmospheric CO₂ concentration that are used to investigate surface exchanges of CO₂ reflect a mixture of influences depending on the location and magnitude of fluxes and on the transport or mixing of air. Uncertainties in estimates of local fossil fuel-derived CO₂ can contribute significant uncertainty to natural and anthropogenic CO₂ flux estimates on subannual and subcontinental scales (Gerbig et al., 2003; Gibert et al., 2007). Reliable techniques for estimating fossil fuel CO₂ or fossil fuel CO₂ emissions need to be developed to serve the expansion of CO₂ flux investigations at these scales (Wofsy and Harriss,

2002). Observation-based estimates of CO₂ emitted by fossil fuel combustion could additionally provide a method for verifying economic emission inventories and government-mandated emissions reductions on regional scales (Levin and Rödenbeck, 2008).

The ratio of ¹⁴C, or radiocarbon, to ¹²C is a nearly perfect tracer of fossil fuel-derived CO₂, as the combustion of million year old fossil carbon produces CO₂ containing only the stable isotopes ¹²C and ¹³C. Addition of CO₂ from fossil sources dilutes the ratio ¹⁴CO₂/¹²CO₂ in the local atmosphere (Suess, 1955), which is typically reported as $\Delta^{14}\text{C}$ in part per thousand deviation from a standard ratio (Stuiver and Polach, 1977). Conversely, respiratory fluxes involve carbon that has been recently fixed, on average, and the calculation of $\Delta^{14}\text{C}$ corrects for mass-dependent fractionation using measurements of ¹³C/¹²C. Emissions from fossil fuel combustion thus add CO₂ with a $\Delta^{14}\text{C}$ of -1000‰ , producing a strongly negative effect on $\Delta^{14}\text{C}$ of CO₂, whereas biospheric exchange does not substantially

*Corresponding author.

e-mail: heather.graven@env.ethz.ch

†Now at: Institute for Biogeochemistry and Pollutant Dynamics, ETH Zurich, Zurich, Switzerland

DOI: 10.1111/j.1600-0889.2009.00421.x

alter $\Delta^{14}\text{C}$ in local CO_2 . By observing differences in $\Delta^{14}\text{C}$ and CO_2 concentration relative to background values, CO_2 added by fossil fuel sources can be distinguished from CO_2 that is added or removed by biospheric sources or sinks using mass balances of CO_2 and ^{14}C (Tans et al., 1979; Levin et al., 1980; Meijer et al., 1996; Takahashi et al., 2002; Levin et al., 2003; Gamnitzer et al., 2006; Turnbull et al., 2006).

A limitation of the ^{14}C method for assessing fossil-fuel emissions is that measurements of $\Delta^{14}\text{C}$ are expensive and require discrete samples of air. Other trace gases related to combustion, mainly CO but also SF_6 and C_2Cl_4 , can be measured with reduced expense and with the possibility of continuous observation. However, quantifying fossil CO_2 present in an air sample with measurements of these gases requires the application of emission ratios that are highly variable, depending on the type of fuel and combustion (EPA, 2006; Rivier et al., 2006). Other techniques combine a priori assumptions of the distribution of surface fossil fuel emissions (e.g., Andres et al., 1996) with transport models to calculate the amount of fossil fuel-derived CO_2 present at a sampling location (e.g., Gurney et al., 2002; Campbell et al., 2007). Such estimates are subject to potentially large uncertainties or errors in atmospheric transport or in assumed emissions (Marland et al., 1999; Rödenbeck et al., 2003; Gurney et al., 2005; Geels et al., 2007).

To investigate the use of $\Delta^{14}\text{C}$ for estimating fossil fuel-derived CO_2 in airborne measurement campaigns, we collected whole air samples for $\Delta^{14}\text{C}$ analysis during vertical profiling of the lower troposphere in rural and urban areas of Colorado, USA, as part of the Airborne Carbon in the Mountains Experiment (ACME) in May and July of 2004. Measurements of $\Delta^{14}\text{C}$ and CO_2 concentration are presented in this paper and used to define a simple mixture of background, biospheric and fossil fuel-derived CO_2 in each sample, enabling the observation of changes in CO_2 added by fossil fuel and biospheric sources with altitude. In situ measurements of CO are also combined with ^{14}C -based estimates of fossil fuel- CO_2 to estimate fossil fuel emission ratios $\text{CO}_2 : \text{CO}$ or R_{ff} , which are used to compare with emission inventory values and to assess the reliability of fossil fuel-derived CO_2 estimated by CO through characterization of variability in R_{ff} .

2. Methods

2.1. Flask sampling and analysis

The ACME campaign used the National Center for Atmospheric Research/National Science Foundation C-130 aircraft. Whole air samples were taken onboard the aircraft using evacuated 5-L spherical glass flasks with a single ground tapered stopcock sealed with Apiezon[®] type N grease. Outside air was sampled from a forward-facing 1/2" stainless steel inlet and flushed through Synflex[®] tubing. No pumps were used; air flowed through the tubing in response to the pressure gradient

between the inlet and exhaust, located beneath and to the rear of the cabin. To sample, a valve was closed downstream and the evacuated flask was opened for approximately 30 s, until it reached the inlet pressure.

Flasks were sampled in May and July 2004, over two areas. One area was a mountainous rural setting near Kremmling, Colorado, a town with a population of approximately 1500 inhabitants, located 100 km to the west of Denver and 40 km to the west of the continental divide at 40.06°N, 106.38°W and 2252 m elevation. The other area was an urban setting near Broomfield, Colorado, located at 39.91°N, 105.12°W and 1728 m elevation, within the Denver metropolitan area which has a population of approximately 2.5 million people. Flasks were collected during vertical ascents and/or descents between a cruising altitude of 5.5–7 km above mean sea level (AMSL) and less than 100 m above ground level (AGL). Vertical profiles were conducted over Kremmling in the morning and over Denver in the morning and afternoon.

Each flask was measured for CO_2 mole ratio in dry air at the Scripps Institution of Oceanography (SIO), using a non-dispersive infrared gas analyser with a precision of $\pm 0.1 \mu\text{mol mol}^{-1}$ or ppm (Keeling et al., 2002). CO_2 was then cryogenically extracted from all of the remaining air in the flask, producing CO_2 samples of 20 $\mu\text{mol C}$ in flasks sampled above 5 km to 45 $\mu\text{mol C}$ in flasks sampled near the surface.

A set of 27 of the CO_2 samples were split approximately in half to enable both stable isotope ratio mass spectrometry (IRMS) and ^{14}C measurement by accelerator mass spectrometry (AMS) in the same sample, 13 samples were used entirely for AMS analysis, and one sample was used entirely for IRMS analysis. IRMS was conducted at SIO using a Micro-Mass Optima dual-inlet mass spectrometer with a precision of $\pm 0.03\%$ (Guenther et al., 2001). For ^{14}C measurements, CO_2 samples were converted to graphite and analysed with AMS at Lawrence Livermore National Laboratory (LLNL) with precision of $\pm 1.7\text{--}2.4\%$, based on the reproducibility of CO_2 extracted from whole-air reference cylinders (Graven et al., 2007; Graven, 2008). We report $^{14}\text{C}/^{12}\text{C}$ ratios using $\Delta^{14}\text{C}$ notation, where the ratios were corrected for radioactive decay between the times of sampling and analysis and for mass-dependent fractionation using $\delta^{13}\text{C}$ (Stuiver and Polach, 1977). To calculate $\Delta^{14}\text{C}$ in the samples that were used only for AMS analysis, we estimated $\delta^{13}\text{C}$ using a spline interpolation between $\delta^{13}\text{C}$ and $1/\text{CO}_2$ measured in other samples taken on the same profile, assuming that the air throughout the sample profile was influenced by CO_2 sources with the same average $\delta^{13}\text{C}$. The observations are listed in tabulated form in the Appendix.

In situ measurements of CO were performed with an Aero-Laser vacuum ultraviolet resonance fluorescence instrument (Gerbig et al., 1999) with 1 s time resolution and precision of ± 3 ppb. In situ measurements of CO_2 used a modified commercial LI-COR 6252 analyser with 1 s time resolution and precision of ± 0.3 ppm. Meteorological and positioning

variables were measured onboard the aircraft and recorded as 1 s averages.

To assess the reproducibility of $\Delta^{14}\text{C}$ and CO_2 in our sampling and analysis methods, we collected pairs of flasks in rapid succession while cruising at 5.5 km AMSL. The first pair was sampled within 2 min on 20 May 2004 and the second pair was sampled within 1.5 min on 20 July 2004. Combining the results for both pairs, the root-mean-square of the standard deviations was 1.9‰ in $\Delta^{14}\text{C}$ and 0.3 ppm in CO_2 , slightly higher than or comparable to the measurement uncertainty in both $\Delta^{14}\text{C}$ and CO_2 . The agreement in these pairs implies that the amount of uncertainty added in processing the samples was negligible.

2.2. Calculating CO_2 source components

CO_2 source components from vegetation and fossil fuel emissions are calculated from simple mass balances. We refer to source components as the amount of CO_2 present in units of CO_2 mole ratio (ppm), not as CO_2 fluxes (i.e. with units of $\text{g m}^{-2} \text{day}^{-1}$).

We take the measured CO_2 mixing ratio (C_{meas}) to be a sum of CO_2 derived from vegetative exchange by photosynthesis and respiration (C_{P} and C_{R}) and fossil fuel combustion (C_{ff}) added to background levels (C_{bg}): $C_{\text{meas}} = C_{\text{P}} + C_{\text{R}} + C_{\text{ff}} + C_{\text{bg}}$. For ^{14}C , we rely on an approximate mass balance for ^{14}C using the sum of the product of the $\Delta^{14}\text{C}$ signature (represented as Δ) and the amount of CO_2 : $C_{\text{meas}} \Delta_{\text{meas}} \approx C_{\text{P}} \Delta_{\text{bg}} + C_{\text{R}} \Delta_{\text{veg}} + C_{\text{ff}} \Delta_{\text{ff}} + C_{\text{bg}} \Delta_{\text{bg}}$.

Since ^{14}C is absent from fossil fuel carbon, Δ_{ff} is -1000‰ , and C_{ff} comprises only CO_2 from fossil fuel combustion. CO_2 added by the combustion of biofuels or biomass are included in C_{R} . Δ_{veg} , the $\Delta^{14}\text{C}$ level in CO_2 respired by terrestrial vegetation, is not well known and may be quite heterogeneous over different species and ecosystems. In previous studies, Δ_{veg} has been estimated with a mean ecosystem residence time of approximately 10 yr (Turnbull et al., 2006) or presumed to be equal to Δ_{bg} , because most of the ecosystem flux comes from a rapidly overturning reservoir (Levin et al., 2003; Gammitzer et al., 2006). As in Levin et al. and Gammitzer et al., we assume here that respired CO_2 has a $\Delta^{14}\text{C}$ content that is the same as the background air, $\Delta_{\text{veg}} = \Delta_{\text{bg}}$. This assumption allows the simple aggregation of respiratory and photosynthetic activity of the local vegetation into $C_{\text{veg}} = C_{\text{P}} + C_{\text{R}}$.

Combining the two mass balance equations and the assumptions for Δ_{ff} and Δ_{veg} , we solve for the two unknowns, C_{ff} and C_{veg} :

$$C_{\text{ff}} = C_{\text{meas}} \frac{\Delta_{\text{bg}} - \Delta_{\text{meas}}}{\Delta_{\text{bg}} + 1000}, \quad (1)$$

$$C_{\text{veg}} = C_{\text{meas}} - C_{\text{bg}} - C_{\text{ff}}. \quad (2)$$

We consider two possible definitions for the background composition: CO_2 and $\Delta^{14}\text{C}$ observed at clean-air stations or CO_2

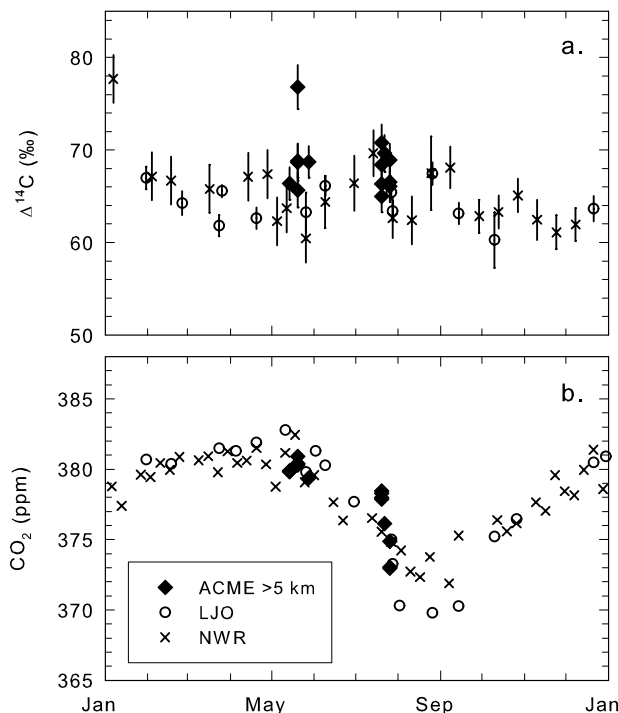


Fig. 1. $\Delta^{14}\text{C}$ (a) and CO_2 mole ratio (b) in ACME flasks sampled above 5 km AMSL (solid diamonds) and in clean-air flasks sampled at La Jolla, California (LJO, circles) and Niwot Ridge, Colorado (NWR, crosses) for 2004. LJO data from the Scripps CO_2 Program (Graven, 2008); NWR CO_2 data from NOAA/ESRL (Conway and Tans, 2004) and NWR $\Delta^{14}\text{C}$ data from Turnbull et al. (2007).

and $\Delta^{14}\text{C}$ measured in the ACME flasks sampled in the free troposphere. Figure 1 shows CO_2 and $\Delta^{14}\text{C}$ measured in ACME flasks sampled above 5 km AMSL and in flasks sampled at two clean-air sampling stations during 2004. Data shown are from the Scripps CO_2 Program at La Jolla, California and from the National Oceanic and Atmospheric Administration's Earth System Research Laboratory (NOAA/ESRL) at Niwot Ridge, Colorado (Conway and Tans, 2004; Turnbull et al., 2007). CO_2 samples from SIO were measured for $\Delta^{14}\text{C}$ at LLNL using similar procedures as the ACME samples; NOAA/ESRL CO_2 samples were measured for $\Delta^{14}\text{C}$ at the Rafter Radiocarbon Laboratory and the University of California, Irvine. Replicate measurements were averaged in Fig. 1.

CO_2 mole ratios in upper air observations during ACME were similar to the clean-air stations, showing most coherence with observations at Niwot Ridge. High-altitude measurements of $\Delta^{14}\text{C}$ appear to be slightly higher ($\sim 3\text{‰}$) than the clean-air stations over the same time period, based on the mean $\Delta^{14}\text{C}$ between May and July in samples from La Jolla ($64.6 \pm 1.4\text{‰}$, where 1.4‰ is the standard deviation), Niwot Ridge ($64.2 \pm 3.0\text{‰}$) and the upper air samples ($67.7 \pm 1.8\text{‰}$). In calculating the mean upper air $\Delta^{14}\text{C}$, we excluded one sample that exhibited exceptionally high $\Delta^{14}\text{C}$ (20 May, 5.5 km AMSL, 76.8‰), over

5‰ higher than any other sample collected during the ACME campaign. A similar positive anomaly was observed at Niwot Ridge on 5 Jan 2004.

The high- $\Delta^{14}\text{C}$ excursions observed in the high-altitude sample and at Niwot Ridge may have resulted from the presence of ^{14}C -enriched air from the stratosphere or by cosmogenic production in the upper troposphere. Anthropogenic production of ^{14}C is unlikely to have affected these samples, since there are no active nuclear power plants in Colorado. Stratospheric air with high- $\Delta^{14}\text{C}$ or cosmogenic production of ^{14}C may also have contributed to the $\sim 3\%$ enhancement in the upper air samples in ACME compared with La Jolla and Niwot Ridge. Turnbull et al. (2007) report good agreement between $\Delta^{14}\text{C}$ observed in 3–5 km AMSL airborne samples over New England and $\Delta^{14}\text{C}$ at Niwot Ridge over May–July 2004, though an enrichment of $\sim 3\%$ is apparent in their high-altitude samples over May–July 2005.

The high-altitude and clean-air station measurements both show short term or synoptic scale variability in C_{bg} and Δ_{bg} . Because variability on this scale could influence the expression of daily surface sources, higher temporal resolution in C_{bg} and Δ_{bg} than monthly or seasonal averages is necessary. Therefore, we used the high-altitude measurements on each vertical profile to define C_{bg} and Δ_{bg} for that profile. For the profile on the morning of 20 May, we did not use the sample with exceptionally high $\Delta^{14}\text{C}$ as the background definition; instead, we used the sample taken at the next highest altitude, 3.7 km AMSL.

We estimated the uncertainty in background CO_2 by the scatter in high-altitude measurements. The standard deviation in CO_2 was ± 0.5 ppm in May and ± 2.3 ppm in July. To estimate the uncertainty in background $\Delta^{14}\text{C}$, we used the difference between the high-altitude $\Delta^{14}\text{C}$ on each profile and the average $\Delta^{14}\text{C}$ at La Jolla and Niwot Ridge between May and July (64.3‰) to account for the possibility that the high-altitude enrichment in $\Delta^{14}\text{C}$ was not representative of background air. The difference between high-altitude and clean-air station $\Delta^{14}\text{C}$ ranged between 1.4‰ and 5.3‰, which contributes ± 0.5 to ± 1.9 ppm uncertainty to the CO_2 source components. The uncertainty from C_{bg} was similar to the uncertainty from Δ_{bg} .

Measurement uncertainty of ± 1.7 – 2.4% in $\Delta^{14}\text{C}$ contributes ± 0.6 – 0.8 ppm to the uncertainty in calculated CO_2 sources. The assumption $\Delta_{\text{veg}} = \Delta_{\text{bg}}$ also contributes uncertainty, which scales with the influence of vegetation. If Δ_{veg} was actually higher than Δ_{bg} , our calculations of C_{veg} are too high and C_{ff} , correspondingly, too low. To estimate the uncertainty contributed by the assignment of Δ_{veg} , we assigned $\Delta_{\text{veg}} = 150\%$ and recalculated C_{veg} and C_{ff} , assuming the photosynthetic sink of CO_2 was 0 ppm in the morning profiles and 8 ppm or smaller in the afternoon profiles. When estimated as the standard deviation between C_{veg} calculated using the two different assumptions for Δ_{veg} , the uncertainty from Δ_{veg} may be as large as 2.8 ppm for the sample with the greatest influence of respiration (55.8 ppm), but averages to 0.3 ppm in May and 0.5 ppm in July.

Overall, the uncertainty in the background values Δ_{bg} and C_{bg} and the AMS measurement precision contribute the most uncertainty to C_{ff} and C_{veg} . We estimate total uncertainty in C_{ff} and C_{veg} for each flask as a quadrature sum of the uncertainty contributed by the CO_2 and $\Delta^{14}\text{C}$ background composition, the measurement uncertainty of CO_2 and $\Delta^{14}\text{C}$ and the uncertainty from Δ_{veg} (Ellison et al., 2000). The total uncertainty in CO_2 source components averaged 1.6 ppm in May and 2.9 ppm in July.

3. Results and discussion

3.1. Rural and urban patterns

Results from nine vertical profiles are shown in Fig. 2. In each profile, the left-hand panel shows CO_2 concentration (flask data in black circles; in situ data in grey lines), the centre panel shows $\Delta^{14}\text{C}$ (diamonds) and the right-hand panel shows the source components of CO_2 (ΔCO_2) as C_{veg} (black bars) and C_{ff} (grey bars). Average uncertainty in source components is shown in the right-hand panel of each profile as a $2\text{-}\sigma$ error bar.

Vertical profiles sampled in the morning around 7 a.m. in the rural area near Kremmling are shown in Figs 2a (20 May 2004) and b (22 July 2004). Very high CO_2 concentration was observed near the surface, with enhancements as large as 55.8 ppm on 22 July. Concurrent $\Delta^{14}\text{C}$ data showed little change from the surface to higher altitude. Calculated C_{veg} and C_{ff} reveal that this CO_2 was almost entirely of biospheric origin (14.1 ± 2.1 and 55.8 ± 4.1 ppm for a and b, respectively), whereas only 1.2 ± 2.1 and 1.6 ± 4.1 ppm were attributed to fossil fuel combustion in air sampled closest to the surface.

High concentrations of biosphere-derived CO_2 near the surface in morning samples reflect the accumulation of respired CO_2 into a stable nocturnal boundary layer (Keeling, 1958; Wofsy et al., 1988). In the mountainous rural area near Kremmling sampled during the ACME campaign, the near-surface concentrations were likely enhanced by surface drainage flows in surrounding mountain valleys (Baldocchi et al., 2000; Pypker et al., 2007). The slight increase in $\Delta^{14}\text{C}$ with altitude suggests that fossil emissions added a small contribution to the biospheric surface level CO_2 enrichment. The quantification of C_{veg} from these profiles can be directly compared to predictions of CO_2 fluxes from biospheric models of the local montane ecosystems that are being pursued by other ACME participants (Schimel et al., 2002).

Figures 2c and d show profiles sampled near 10 a.m., above the large urban area of Denver on 20 May and 20 July 2004. More modest enhancements in CO_2 were observed near the surface compared with the rural profiles sampled earlier in the morning. On 20 May, fossil fuel burning and local vegetation made roughly equal contributions to the elevated CO_2 in the sample collected at the lowest altitude ($C_{\text{ff}} = 4.0 \pm 1.9$ ppm and $C_{\text{veg}} = 3.5 \pm 1.9$ ppm). Observations on 20 July showed a

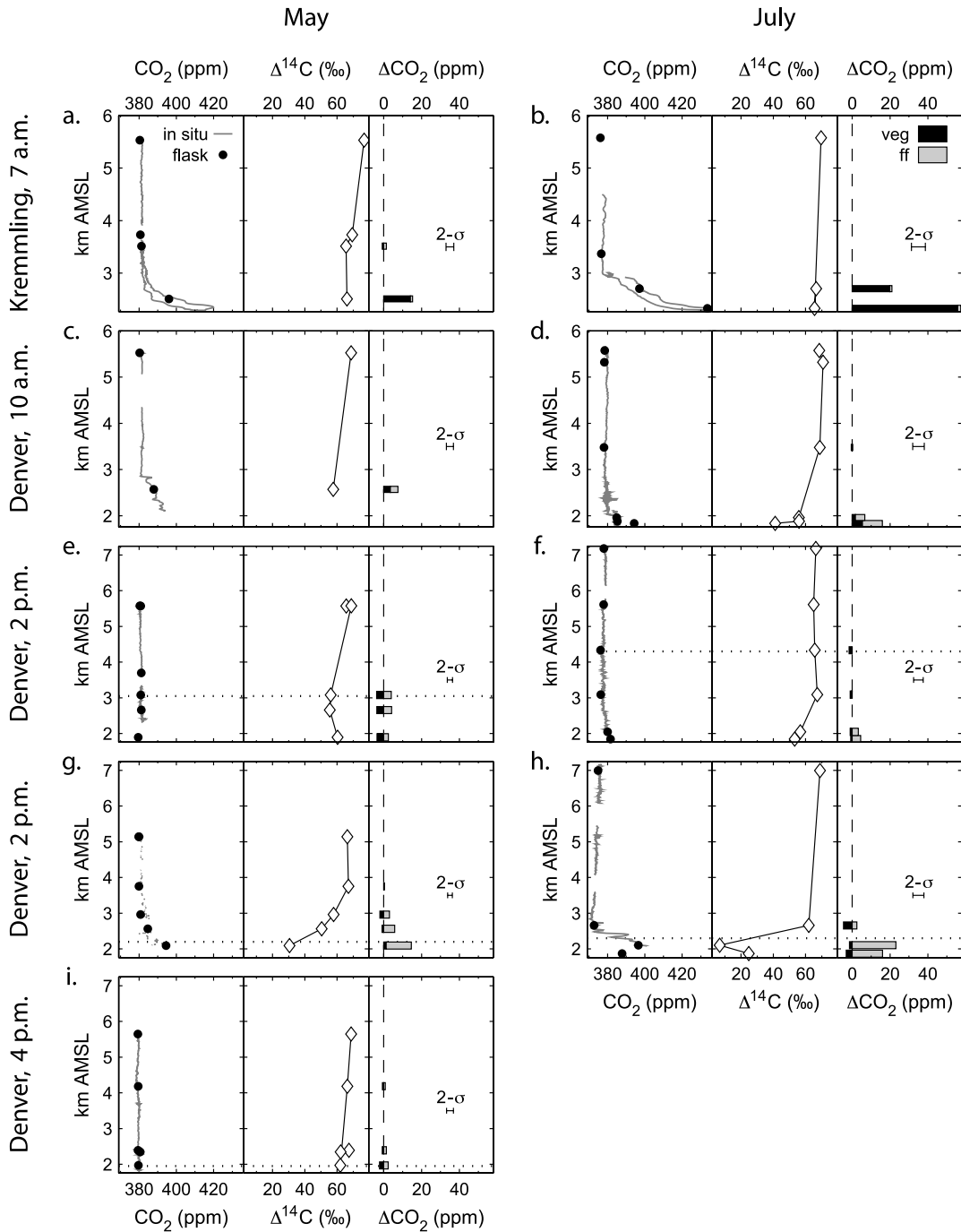


Fig. 2. Vertical profiles of CO_2 concentration (left-hand panel: flask data in black circles, in situ data in grey lines), $\Delta^{14}\text{C}$ (centre panel, diamonds), and the amount of CO_2 added (ΔCO_2 , right panel) as C_{veg} (black bars) and C_{ff} (grey bars). Altitude is given in km AMSL, where the ground level is at the base of the plot (2.27 km AMSL over Kremmling and 1.76 km AMSL over Denver). Plots (a) and (b) show profiles sampled above Kremmling, Colorado at 7 a.m. on 20 May and 22 July 2004, respectively. Plots (c) and (d) show profiles sampled above Denver, Colorado at 10 a.m. on 20 May and 20 July 2004, respectively. Plots (e), (f), (g), (h) and (i) show profiles sampled above Denver, Colorado at 2 p.m. on 20 May, 20 July, 14 May and 26 July and 4 p.m. on 28 May 2004, respectively. The dotted horizontal lines in (e), (f), (g), (h) and (i) show the approximate altitude at the top of the boundary layer for each day, as estimated by the vertical profile of potential temperature. The errorbar in the right-hand panel shows the average total uncertainty in ΔCO_2 for each profile. Uncertainties in CO_2 and $\Delta^{14}\text{C}$ are smaller than the symbol size.

larger component of fossil fuel-derived CO_2 (10.5 ± 3.1 ppm) than biospheric CO_2 (5.4 ± 3.1 ppm). C_{veg} was substantial and comparable in magnitude to C_{ff} in these morning samples from the urban Denver region, similar to results from ground-based, nighttime $\delta^{13}\text{C}$ and $\delta^{18}\text{O}$ measurements in CO_2 from Salt Lake City, Utah (Pataki et al., 2003).

Profiles sampled above Denver at approximately 2 p.m. on 20 May, 20 July, 14 May and 26 July and at 4 p.m. on 28 May are shown in Figs 2e, f, g, h and i, respectively, with the addition of a dotted line showing the vertical extent of the turbulent planetary boundary layer (PBL). The top of the boundary layer was estimated by the altitude where the potential temperature began increasing with height (Henne et al., 2004). The afternoon profiles can be grouped into days that had deep boundary layers (20 May and 20 July) and days that had shallow boundary layers (14 May, 26 July and 28 May).

Profiles sampled in deep boundary layers of approximately 1.3–2.5 km depth are shown in Figs 2e and f. Low variability in CO_2 and $\Delta^{14}\text{C}$ and small amounts of C_{ff} and C_{veg} were observed through these deep boundary layers. Relatively uniform CO_2 concentration is expected, as a deep PBL allows surface fluxes of CO_2 to be diluted with a large volume of air (Wofsy et al., 1988). The profile of $\Delta^{14}\text{C}$ from 20 May (Fig. 2g) indicates that compensation of fossil fuel emissions and biospheric CO_2 uptake can additionally contribute to low deviation from background CO_2 levels. C_{veg} was consistently -3.7 ± 1.4 ppm and C_{ff} was between 2.5 and 4.2 ± 1.4 ppm for the three samples collected within the boundary layer. On 20 July, biospheric influence in low altitude samples was small, -0.8 ± 2.5 ppm and -1.1 ± 2.5 ppm, and not significantly different from zero (Fig. 2f) whereas fossil fuel CO_2 of 4.4 ± 2.5 ppm and 3.2 ± 2.5 ppm caused a slight increase in CO_2 and decrease in $\Delta^{14}\text{C}$ near the surface.

Comparison of Figs 2c and e and Figs 2d and f shows differences between morning and afternoon profiles sampled on the same day above Denver. On 20 May (Figs 2c and e), $\Delta^{14}\text{C}$ was extremely consistent at high and low altitudes between morning and afternoon. The mole ratio of CO_2 remained constant at high altitudes throughout the day whereas in the afternoon, elevated CO_2 near 1 km AGL disappeared, indicating C_{ff} present at this level was similar between morning and afternoon whereas C_{veg} changed from positive (3.5 ± 1.8 ppm) to negative (-3.7 ± 1.4 ppm). Similarly, on 20 July, the upper air composition was largely constant and the elevation in CO_2 near the surface was reduced in the afternoon compared with the morning. C_{veg} had again changed from positive in the morning to negative or near zero, yet in this case, C_{ff} over Denver was also reduced in the afternoon.

Profiles sampled in shallow boundary layers of 200–500 m are shown in Figs 2g–i. On 14 May (Fig. 2g), CO_2 decreased uniformly with height whereas $\Delta^{14}\text{C}$ increased uniformly with height. Additions of CO_2 were mainly caused by fossil fuel combustion, yet vegetative exchange also appeared to influence CO_2

up to 1 km AGL. Above the PBL C_{veg} was negative, indicating that upper level air experienced net photosynthetic uptake of CO_2 (-2.1 ± 1.1 ppm at 3 km AMSL), which likely represents a residual layer with influence from the previous afternoon. C_{veg} was positive within the boundary layer, indicating a net source of biospheric CO_2 had recently influenced low level air (1.3 ± 1.3 ppm). Vertical gradients observed on 26 July (Fig. 2h) were complex: CO_2 increased by ~ 10 ppm from the surface to ~ 250 m AGL, then decreased to a minimum at 1–1.5 km AGL. Varying amounts of C_{ff} present at each level accounted for most of the change in CO_2 , whereas C_{veg} indicated biospheric uptake in air at all levels, ranging from -1.4 to -4.6 ± 2.9 ppm. The profile on 28 May (Fig. 2i) appeared to sample a PBL of only ~ 200 m depth, yet $\Delta^{14}\text{C}$ and CO_2 expressed relatively little change between the air within and above the boundary layer compared with the profiles in Figs 2g and h. C_{ff} was found to be 2.4 ± 1.8 ppm just below the top of the boundary layer, and an average of 1.4 ± 1.8 ppm in the two samples collected just above it, whereas C_{veg} was -2.2 ± 1.8 and -0.8 ± 1.8 ppm. The profiles in Figs 2g–i show that the vertical distribution of CO_2 , $\Delta^{14}\text{C}$ and the source components C_{ff} and C_{veg} were highly variable in shallow boundary layers above Denver.

C_{ff} was not generally correlated with wind direction in the afternoon profiles. Wind direction was westerly or southerly in high-altitude air whereas wind from all sectors was observed at low levels. Wind direction was not consistent between the samples with the highest C_{ff} near the surface: the wind was westerly (275°) on 14 May, southeasterly (140°) on 20 July and easterly (100°) on 26 July. Wind direction also cannot explain the difference in the C_{ff} between the two low-level samples on 26 July (Fig. 2h), as the wind direction was $\sim 100^\circ$ from the surface up to 2.8 km AMSL. However, on 20 May (Fig. 2e), the vertical changes in C_{ff} were analogous to vertical changes in wind direction. C_{ff} was higher in the two mid-level samples than in the near-surface sample; at the same time, wind direction was northeasterly in the two mid-level samples but southeasterly in the near-surface sample.

3.2. Correlation of C_{ff} with CO

Measurements of another product of fossil fuel combustion, CO, are often used to estimate fossil-derived CO_2 (Bakwin et al., 1998; Gerbig et al., 2003; Turnbull et al., 2006; Gammitzer et al., 2006; Levin and Karstens, 2007). Relative production of CO_2 compared with CO (R_{ff}) greatly depends on the type of fuel and the type of combustion; for the same amount of CO_2 production, CO emissions from automobiles are roughly 300 times larger than emissions from stationary sources using solid, liquid or gaseous fuels (EPA, 2006), resulting in lower $C_{\text{ff}} : \text{CO}$ in areas where transportation emissions contribute more to C_{ff} . Spatial and temporal variability in combustion and fuel type may therefore result in large variability in R_{ff} .

Table 1. Molar C_{ff} :CO ratios and reciprocal CO: C_{ff} ratios from observations and inventories for several locations in the US, including observations from ACME

Date and time	Location	C_{ff} :CO	CO: C_{ff} ($\times 10^3$)	Reference
20 May 2004, 7 am	Kremmling, Col.	56 ± 31	18 ± 10	This study
20 May 2004, 2 pm	Denver, Col.	50 ± 5	20 ± 2	This study
28 May 2004, 2 pm	Denver, Col.	37 ± 11	27 ± 8	This study
20 July 2004, 10 am	Denver, Col.	69 ± 10	14 ± 2	This study
26 July 2004, 2 pm	Denver, Col.	74 ± 18	14 ± 3	This study
May 1994–1996 average	Harvard Forest, Mass.	45 ± 3	22 ± 2	Potosnak, 1999
July 1994–1996 average	Harvard Forest, Mass.	34 ± 6	29 ± 5	Potosnak, 1999
20 January 2004	Niwot Ridge, Col.	147 ± 48	7 ± 2	Turnbull, 2006
2 March 2004	Niwot Ridge, Col.	85 ± 40	12 ± 6	Turnbull, 2006
August 2000	North American survey	30 ± 9	33 ± 10	Gerbig, 2003
2004 average	EPA inventory, US average	43	23	EPA, 2006
2001 average	DOE inventory, Col. average	31	32	Blasing, 2004
2002 average	Vulcan inventory, Col. average	53	19	Gurney, 2008

We use the $\Delta^{14}\text{C}$ -derived C_{ff} to estimate ratios of C_{ff} :CO by geometric mean regressions with CO concentration measured in situ, averaged over the ~ 30 s flask sampling period. Regressions were calculated between C_{ff} and CO, without specifying or subtracting background CO concentrations. This method essentially assigns background CO to be the x -intercept of the regression.

Five vertical profiles had at least three measurements of both C_{ff} and CO, which spanned a range of 30 ppb or more in CO. Table 1 lists the time and location of these high-variability profiles, the molar C_{ff} :CO ratio with the uncertainty in the fitted regression coefficient and the reciprocal CO: C_{ff} , including a factor of 10^3 (equivalent to nmol mol^{-1} CO: $\mu\text{mol mol}^{-1}$ CO₂ or ppb CO:ppm CO₂). Table 1 also summarizes ratios observed in previous studies and reported in emissions inventories.

R_{ff} observed during ACME ranged from 37 to 74. Observed ratios were highly consistent on 20 May (56 ± 31 and 50 ± 5) and between 20 and 26 July (69 ± 10 and 74 ± 18), whereas R_{ff} for 28 May was much lower (37 ± 11). The ratios broadly agree within the uncertainties in fitted regression coefficients though the values span a factor of two. For these estimates, uncertainty in C_{ff} and heterogeneity in emission types contribute to uncertainties in regression coefficients.

CO is also emitted in biofuel or biomass combustion and is created and removed via photochemical reactions involving the hydroxyl radical. Approximately 3% of CO emitted by fuel combustion is derived from biofuels in Colorado, similar to the US average (APCD, 2005; EPA, 2006). The contribution of these non-fossil emissions to the observed enhancements of CO during ACME may introduce an error of 0 to -2 in the estimates of R_{ff} , which is much smaller than the regression uncertainties. CO₂ emitted by biofuel combustion is allocated to C_{veg} and therefore does not affect the calculation of R_{ff} . Biomass burning did not appear to influence air that was sampled in the ACME campaign, as there was relatively good visibility and no apparent smoke

plumes. The influence of photochemistry on CO concentrations was computed at locations where flasks were sampled in July, as in Campbell et al. (2007). Photochemical effects were found to be a small net sink for CO, averaging -3 ± 3 ppb with vertical gradients of 5 ppb or less, which could also introduce only a small error of 0 to -2 to R_{ff} .

The average combustion ratio was higher in July (72) than in May (48). This change is opposite to that observed in Harvard Forest over 1994–1996, where the average ratio decreased from May (45) to July (34) (Potosnak et al., 1999, Table 1). Differences in the seasonal change in C_{ff} :CO between these two areas may be due to differing local emission types, photochemical effects in Harvard Forest and/or unrepresentative sampling.

Two observations of C_{ff} :CO in ground-based flask samples at Niwot Ridge, Colorado in winter 2004 showed much higher ratios, 147 ± 48 and 85 ± 40 (Turnbull et al., 2006, Table 1). The large discrepancy could reflect a seasonal change in combustion and fuel type in Colorado, perhaps due to an increase in the relative proportion of transportation to total emissions in summer.

Observed C_{ff} :CO ratios overlap with the US Environmental Protection Agency inventory average for 2004, 43 (EPA, 2006), yet four of five observations were higher than 43. The US Department of Energy inventory estimate of C_{ff} :CO for Colorado for 2001 is 31 (Blasing et al., 2004), lower than all observations. Another emissions compilation for 2002 by Gurney et al. (2008) indicates a higher state-wide average, 53.

$\Delta^{14}\text{C}$ measurements suggest that actual C_{ff} :CO in these sampling locations was higher than the inventory estimates, as suggested by Turnbull et al. (2006). Studies utilizing inventory estimates of C_{ff} :CO together with CO measurements to estimate C_{ff} could then underestimate C_{ff} and, as a result, underestimate biospheric uptake of CO₂. Inventories may include errors in the relative fraction of different fuel types or combustion methods

used in Colorado, or the combustion sources may be too heterogeneous to be represented by a state-wide or nation-wide average. Recent, high spatial resolution estimates of CO_2 emissions suggest that R_{ff} varies by 300% among the six counties that surround the ACME sampling area (Gurney et al., 2008). Observations and inventories of $C_{\text{ff}}:\text{CO}$ in Europe are generally higher than the US, 91-114 (Meijer et al., 1996; Braud et al., 2004; Gamnitzer et al., 2006), reflecting the smaller proportion of CO_2 emissions contributed by automobiles and the greater prevalence of diesel combustion engines, which emit proportionally less CO (EPA, 2006).

The $C_{\text{ff}}:\text{CO}$ ratios summarized in Table 1 span a factor of 4 for several dates and locations within the US, demonstrating that the use of CO to trace C_{ff} is highly uncertain when the $C_{\text{ff}}:\text{CO}$ ratio is not accurately known. A useful application would combine in situ CO measurements with regular observation of $\Delta^{14}\text{C}$ in flask air to characterize local R_{ff} and to account for temporal or spatial variability in emission type (Gamnitzer et al., 2006; Levin and Karstens, 2007).

4. Summary

Observation of $\Delta^{14}\text{C}$ in CO_2 in vertical profiles of the lower troposphere revealed patterns of CO_2 source components in urban and rural locations that were influenced by vertical mixing. Early morning samples collected in rural Colorado exhibited large enhancements in CO_2 concentration near the surface that were characterized by $\Delta^{14}\text{C}$ to be almost entirely biospheric in origin. Samples collected in urban areas showed varying mixtures of C_{veg} and C_{ff} , including net biospheric uptake of CO_2 .

This study highlights the capability of $\Delta^{14}\text{C}$ observations to separate fossil fuel and biospheric influences on CO_2 . Uncertainty in C_{veg} and C_{ff} by $\Delta^{14}\text{C}$ is limited mainly by measurement uncertainty and by the uncertainty in characterizing background levels of CO_2 and $\Delta^{14}\text{C}$. Variability in CO_2 source components of ± 1.1 ppm can presently be detected with $\Delta^{14}\text{C}$ measurement uncertainty of $\pm 1.7\text{‰}$, when background levels of $\Delta^{14}\text{C}$ and CO_2 concentration are known to $\pm 2.0\text{‰}$ and ± 0.5 ppm.

Profiles sampled in the afternoon demonstrate that $\Delta^{14}\text{C}$ provides unique insight into the vertical propagation and mixing of particular sources of CO_2 . Airborne measurement of $\Delta^{14}\text{C}$ allows the components C_{veg} and C_{ff} to be characterized from the surface through the boundary layer, greatly augmenting observations of CO_2 concentration.

Together with atmospheric transport modelling, similar airborne measurements of $\Delta^{14}\text{C}$ could be applied to the investigation of some of the main sources of uncertainty in continental-scale carbon budgets: biospheric exchange rates, vertical mixing of surface fluxes and the estimation of industrial CO_2 emissions (Marland et al., 1999; Schimel et al., 2001; Gurney et al., 2002; Stephens et al., 2007).

5. Acknowledgments

The Carbon in the Mountains experiment was funded by National Science Foundation Award EAR-0321918. The National Center for Atmospheric Research is sponsored by the National Science Foundation. H.D.G. received support from the UC Office of the President and a NASA ESS Fellowship. A portion of this work was performed under the auspices of the US Department of Energy by the University of California, Lawrence Livermore National Laboratory under Contract No. W-7405-Eng-48. Radiocarbon analyses were funded by grants from NOAA's Office of Global Programs (NA05OAR4311166) and LLNL's Directed Research and Development programme (06-ERD-031) to T.P.G. Alane Bollenbacher conducted CO_2 and stable isotope analyses. Guy Emanuele assisted with CO_2 extractions. Design and construction of the flask sampling apparatus was aided by NCAR Research Aviation Facility staff, David Moss, Bill Paplawsky and Adam Cox. Design and analysis work at the Scripps Institution of Oceanography was supported by the US National Science Foundation grants ATM-0632770 and the Office of Science (BER), US Department of Energy, through Contracts No. DE-FG02-04ER63898 and -07ER64632. This research was also presented in H.D.G.'s doctoral dissertation at the University of California, San Diego, USA, 2008.

6. Appendix A

Tabulated data for flasks sampled during ACME: date, local time (in Mountain Daylight Time), longitude, latitude, elevation above mean sea level, wind direction, CO₂ mole ratio, $\Delta^{14}\text{C}$ with measurement uncertainty, $\delta^{13}\text{C}$ and mean CO concentration. Starred $\delta^{13}\text{C}$ were estimated by spline interpolation between $\delta^{13}\text{C}$ and $1/\text{CO}_2$ observed in flasks from the same profile. C_{ff} and C_{veg} were calculated by eqs. (1) and (2). σ_C indicates the total uncertainty in C_{ff} and C_{veg} for each flask sample as described in Section 2.2. Individual profiles are separated by horizontal lines. Samples designated as “background” are italicized.

Date	Time (MDT)	Lon (°W)	Lat (°N)	AMSL (km)	Wind (°)	CO ₂ (ppm)	$\Delta^{14}\text{C}$ (‰)	$\delta^{13}\text{C}$ (‰)	CO (ppb)	C_{ff} (ppm)	C_{veg} (ppm)	σ_C (ppm)
14-May-04	14:09	105.10	40.24	5.140	273	379.90		−8.200				
<i>14-May-04</i>	<i>14:11</i>	<i>105.00</i>	<i>40.09</i>	<i>5.142</i>	<i>278</i>	<i>379.82</i>	<i>66.4 ± 1.8</i>	<i>−8.20*</i>				
14-May-04	14:16	105.12	40.05	3.751	268	379.88	67.0 ± 2.0	−8.20*		−0.2	0.3	1.2
14-May-04	14:20	105.31	40.08	2.961	238	380.79	57.9 ± 1.7	−8.25*		3.0	−2.1	1.1
14-May-04	14:25	105.26	39.81	2.562	208	384.70	50.4 ± 2.1	−8.49*		5.8	−0.9	1.3
14-May-04	14:28	105.19	39.94	2.094	274	394.45	30.5 ± 1.9	−9.052		13.3	1.3	1.3
20-May-04	7:08	106.49	40.28	5.529	220	380.40	76.8 ± 2.4	−8.376	107.9			
<i>20-May-04</i>	<i>7:13</i>	<i>106.25</i>	<i>40.11</i>	<i>3.732</i>	<i>207</i>	<i>380.73</i>	<i>69.4 ± 1.8</i>	<i>−8.38*</i>	<i>111.4</i>			
20-May-04	7:19	106.34	40.05	2.511	151	396.03	66.1 ± 1.9	−8.967	137.6	1.2	14.1	2.1
20-May-04	7:22	106.39	40.14	3.513	198	381.28	65.6 ± 1.7	−8.39*	116.3	1.4	−0.8	2.0
<i>20-May-04</i>	<i>10:05</i>	<i>105.43</i>	<i>39.60</i>	<i>5.525</i>	<i>217</i>	<i>380.28</i>	<i>68.7 ± 2.0</i>	<i>−8.37*</i>	<i>110.4</i>			
20-May-04	10:10	105.24	39.95	2.572	197	387.82	57.6 ± 2.2	−8.574	181.9	4.0	3.5	1.9
<i>20-May-04</i>	<i>14:23</i>	<i>106.07</i>	<i>40.31</i>	<i>5.570</i>	<i>205</i>	<i>380.89</i>	<i>65.7 ± 1.9</i>	<i>−8.20*</i>	<i>103.6</i>			
<i>20-May-04</i>	<i>14:25</i>	<i>106.00</i>	<i>40.24</i>	<i>5.579</i>	<i>205</i>	<i>380.40</i>	<i>68.8 ± 1.8</i>	<i>−8.20*</i>	<i>104.2</i>			
20-May-04	14:32	105.56	39.83	3.696	155	381.18			196.5			
20-May-04	14:35	105.39	39.77	3.078	78	380.92	56.0 ± 1.9	−8.184	193.2	4.0	−3.7	1.4
20-May-04	14:37	105.26	39.82	2.657	64	381.2	55.5 ± 1.9	−8.20*	179.2	4.2	−3.7	1.4
20-May-04	14:41	105.15	39.93	1.894	111	379.52	60.3 ± 2.1	−8.229		2.5	−3.6	1.4
<i>28-May-04</i>	<i>15:45</i>	<i>105.26</i>	<i>40.18</i>	<i>5.648</i>	<i>221</i>	<i>379.37</i>	<i>68.7 ± 1.7</i>	<i>−8.300</i>	<i>105.8</i>			
28-May-04	15:51	105.27	39.91	4.186	222	379.50	66.3 ± 1.7	−8.207	127.6	0.9	−0.7	1.8
28-May-04	16:01	104.85	39.61	1.968	194	379.57	61.9 ± 1.7	−8.210	143.4	2.4	−2.2	1.8
28-May-04	16:05	104.97	39.57	2.390	210	379.43	67.3 ± 1.7	−8.249	117.6	0.5	−0.4	1.8
28-May-04	16:08	105.09	39.72	2.343	136	380.58	62.2 ± 1.7	−8.286	181.5	2.3	−1.1	1.8
<i>20-Jul-04</i>	<i>9:26</i>	<i>105.32</i>	<i>39.53</i>	<i>5.574</i>	<i>294</i>	<i>378.44</i>	<i>68.4 ± 1.8</i>	<i>−7.94*</i>	<i>83.7</i>			
<i>20-Jul-04</i>	<i>9:27</i>	<i>105.26</i>	<i>39.54</i>	<i>5.322</i>	<i>293</i>	<i>378.29</i>	<i>70.8 ± 2.0</i>	<i>−8.019</i>	<i>84.8</i>			
20-Jul-04	9:30	105.29	39.50	3.480	339	378.09	68.9 ± 1.9	−8.145		0.3	−0.5	3.1
20-Jul-04	9:41	104.86	39.62	1.963	316	384.82	55.8 ± 1.7	−8.442	167.0	5.0	1.5	3.0
20-Jul-04	9:42	104.85	39.56	1.883	298	385.21	55.9 ± 1.7	−8.459	187.3	4.9	1.9	3.0
20-Jul-04	9:55	105.08	39.89	1.835	129	394.29	41.1 ± 1.7	−8.943	224.4	10.5	5.4	3.1
20-Jul-04	13:34	105.14	39.92	1.843	186	381.59	53.3 ± 1.7	−8.280	86.1	4.4	−0.8	2.5
20-Jul-04	13:35	105.16	39.96	2.047	140	380.03	56.7 ± 1.7	−8.186	86.4	3.2	−1.1	2.5
20-Jul-04	13:38	105.12	40.06	3.090	122	376.29	67.2 ± 1.7	−8.056	85.0	−0.5	−1.1	2.5
20-Jul-04	13:41	105.24	39.97	4.333	325	376.25	65.7 ± 1.7	−8.035	83.5	0.0	−1.7	2.5
<i>20-Jul-04</i>	<i>13:44</i>	<i>105.46</i>	<i>39.90</i>	<i>5.614</i>	<i>308</i>	<i>377.86</i>	<i>65.0 ± 1.7</i>	<i>−8.195</i>	<i>77.5</i>			
<i>20-Jul-04</i>	<i>13:51</i>	<i>105.95</i>	<i>39.74</i>	<i>7.180</i>	<i>245</i>	<i>377.98</i>	<i>66.3 ± 1.7</i>	<i>−8.19*</i>	<i>78.0</i>			
<i>22-Jul-04</i>	<i>6:49</i>	<i>106.00</i>	<i>40.02</i>	<i>5.576</i>	<i>295</i>	<i>376.14</i>	<i>69.6 ± 2.0</i>	<i>−8.172</i>	<i>93.9</i>			
22-Jul-04	6:53	106.14	39.99	3.369	335	376.64						
22-Jul-04	6:57	106.36	40.05	2.330	90	433.55	65.6 ± 1.7	−10.318	96.1	1.6	55.8	4.1
22-Jul-04	6:57	106.43	40.07	2.706	138	397.09	66.6 ± 2.0	−9.027	97.5	1.1	19.8	3.2
26-Jul-04	13:30	105.14	39.92	1.866	103	387.72	24.8 ± 2.0	−8.638	369.2	16.0	−3.2	2.9
26-Jul-04	13:30	105.17	39.95	2.104	100	396.53	6.7 ± 1.8	−9.025	388.9	23.1	−1.4	2.9
26-Jul-04	13:32	105.17	40.01	2.657	119	372.75	61.9 ± 2.0	−7.962		2.4	−4.6	2.9
<i>26-Jul-04</i>	<i>13:45</i>	<i>106.08</i>	<i>40.02</i>	<i>6.994</i>	<i>251</i>	<i>374.88</i>	<i>68.9 ± 1.7</i>	<i>−8.04*</i>	<i>103.9</i>			

References

- Andres, R. J., Marland, G., Fung, I. and Matthews, E. 1996. A $1^\circ \times 1^\circ$ distribution of carbon dioxide emissions from fossil fuel consumption and cement manufacture, 1950–1990. *Global Biogeochem. Cycles* **54**, 419–429.
- Air Pollution Control Division (APCD) 2005. *Colorado Air Quality Data Report, 2004*, Colorado Department of Public Health and Environment, Denver.
- Bakwin, P. S., Tans, P. P., Hurst, D. F. and Zhao, C. 1998. Measurements of carbon dioxide on very tall towers: results of the NOAA/CMDL program. *Tellus* **50B**, 401–415.
- Baldocchi, D., Finnigan, J., Wilson, K., Paw U, K. T. and Falge, E. 2000. On measuring net ecosystem carbon exchange over tall vegetation on complex terrain. *Bdry-Layer Meteorol.* **96**, 257–291.
- Blasing, T. J., Broniak, C. T. and Marland, G. 2004. Estimates of annual fossil-fuel CO_2 emitted for each state in the U.S.A. and the District of Columbia for each year from 1960 through 2001. In: *Trends: A Compendium of Data on Global Change*, Carbon Dioxide Information Analysis Center, Oak Ridge National Laboratory, US Department of Energy, Oak Ridge, TN.
- Braud, H., Bousquet, P. and Ramonet, M. 2004. CO/CO_2 ratio in urban atmosphere: example of the agglomeration of Paris, France. *Notes des Activités Instrumentales* Volume 42, Institut Pierre Simon Laplace, Paris.
- Campbell, J. E., Carmichael, G. R., Tang, Y., Chai, T., Vay, S. A. and co-authors. 2007. Analysis of anthropogenic CO_2 signal in ICARTT using a regional chemical transport model and observed tracers. *Tellus* **59B**, 199–210.
- Conway, T. J. and Tans, P. P. 2004. Atmospheric carbon dioxide mixing ratios from the NOAA/CMDL Carbon Cycle Cooperative Global Air Sampling Network. In: *Trends: A Compendium of Data on Global Change*, Carbon Dioxide Information Analysis Center, Oak Ridge National Laboratory, US Department of Energy, Oak Ridge, TN.
- Ellison, S. L. R., Rosslein, M. and Williams, A., eds 2000. *EURACHEM/CITAC Guide: Quantifying Uncertainty in Analytical Measurement* 2nd Edition. London.
- Environmental Protection Agency (EPA) 2006. *Inventory of U.S. Greenhouse Gas Emissions and Sinks: 1990–2004*, Washington.
- Gammitzer, U., Karstens, U., Kromer, B., Neubert, R. E. M., Meijer, H. A. J. and co-authors. 2006. Carbon monoxide: A quantitative tracer for fossil fuel CO_2 ? *J. Geophys. Res.* **111**, D22302.
- Geels, C., Gloor, M., Ciais, P., Bousquet, P., Peylin, P. and co-authors. 2007. Comparing atmospheric transport models for future regional inversions over Europe - Part 1: mapping the atmospheric CO_2 signals. *Atmos. Chem. Phys.* **7**, 3461–3479.
- Gerbig, C., Schmitgen, S., Kley, D., Volz-Thomas, A., Dewey, K. and co-authors. 1999. An improved fast-response vacuum-UV resonance fluorescence CO instrument. *J. Geophys. Res.* **104**, 1699–1704.
- Gerbig, C., Lin, J. C., Wofsy, S. C., Daube, B. C., Andrews, A. E. and co-authors. 2003. Toward constraining regional-scale fluxes of CO_2 with atmospheric observations over a continent: 2. analysis of COBRA data using a receptor-oriented framework. *J. Geophys. Res.* **108**(D24), 4757.
- Gibert, F., Schmidt, M., Cuesta, J., Ciais, P., Ramonet, M. and co-authors 2007. Retrieval of average CO_2 fluxes by combining in situ CO_2 measurements and backscatter lidar information. *J. Geophys. Res.* **112**, D10301.
- Graven, H. D. 2008. *Advancing the Use of Radiocarbon in Studies of Global and Regional Carbon Cycling with High Precision Measurements of ^{14}C in CO_2 from the Scripps CO_2 Program*. PhD Thesis. Scripps Institution of Oceanography, University of California, San Diego, USA.
- Graven, H. D., Guilderson, T. P. and Keeling, R. F. 2007. Methods for high-precision ^{14}C AMS measurement of atmospheric CO_2 at LLNL. *Radiocarbon* **49**, 349–356.
- Guenther, P. R., Bollenbacher, A. F., Keeling, C. D., Stewart, E. F. and Wahlen, M. 2001. Calibration methodology for the Scripps $^{13}\text{C}/^{12}\text{C}$ and $^{18}\text{O}/^{16}\text{O}$ stable isotope program, 1996–2000. *A Report Prepared for the Global Environmental Monitoring Program of the World Meteorological Organization*, Scripps Institution of Oceanography.
- Gurney, K. R., Law, R. M., Denning, A. S., Rayner, P. J., Baker, D. and co-authors. 2002. Towards robust regional estimates of CO_2 sources and sinks using atmospheric transport models. *Nature* **415**, 626–30.
- Gurney, K., Chen, Y., Maki, T., Kawa, S., Andrews, A. and co-authors. 2005. Sensitivity of atmospheric CO_2 inversions to seasonal and interannual variations in fossil fuel emissions. *J. Geophys. Res.* **110**, D10308.
- Gurney, K., Seib, B., Ansley, W., Mendoza, D., Fischer, M. and co-authors. 2008. *The Vulcan Inventory, version 1.0*. Purdue University. Available at: <http://www.purdue.edu/eas/carbon/vulcan/research.html>.
- Henne, S., Furger, M., Nyeki, S., Steinbacher, M., Neininger, B. and co-authors. 2004. Quantification of topographic venting of boundary layer air to the free troposphere. *Atmos. Chem. Phys.* **4**, 497–509.
- Keeling, C. D. 1958. The concentration and isotopic abundances of atmospheric carbon dioxide in rural areas. *Geochimica Cosmochimica Acta* **13**, 322–334.
- Keeling, C. D., Guenther, P. R., Emanuele, G., Bollenbacher, A. F. and Moss, D. J. 2002. Scripps Reference Gas Calibration System for Carbon Dioxide-in-Nitrogen and Carbon Dioxide-in-Air Standards: Revision of 1999, *A Report Prepared for the Global Environmental Monitoring Program of the World Meteorological Organization*, Scripps Institution of Oceanography.
- Levin, I. and Karstens, U. 2007. Inferring high-resolution fossil fuel CO_2 records at continental sites from combined $^{14}\text{CO}_2$ and CO observations. *Tellus* **59B**, 245–250.
- Levin, I. and Rödenbeck, C. 2008. Can the envisaged reductions of fossil fuel CO_2 emissions be detected by atmospheric observations? *Naturwissenschaften* **95**, 203–208.
- Levin, I., Munnich, K. O. and Weiss, W. 1980. The effect of anthropogenic CO_2 and ^{14}C sources on the distribution of ^{14}C in the atmosphere. *Radiocarbon* **22**, 379–391.
- Levin, I., Kromer, B., Schmidt, M. and Sartorius, H. 2003. A novel approach for independent budgeting of fossil fuel CO_2 over Europe by $^{14}\text{CO}_2$ observations. *Geophys. Res. Lett.* **30**(23), 2194.
- Marland, G., Brenkert, A. and Olivier, J. 1999. CO_2 from fossil fuel burning: a comparison of ORNL and EDGAR estimates of national emissions. *Environ. Sci. Policy* **2**, 265–273.
- Meijer, H. A. J., Smid, H. M., Perez, E. and Keizer, M. G. 1996. Isotopic characterization of anthropogenic CO_2 emissions using isotopic and radiocarbon analysis. *Phys. Chem. Earth* **21**, 483–487.

- Pataki, D. E., Bowling, D. R. and Ehleringer, J. R. 2003. Seasonal cycle of carbon dioxide and its isotopic composition in an urban atmosphere: Anthropogenic and biogenic effects. *J. Geophys. Res.* **108**, 4735.
- Potosnak, M. J., Wofsy, S. C., Denning, A. S., Conway, T. J., Munger, J. W. and co-authors. 1999. Influence of biotic exchange and combustion sources on atmospheric CO₂ concentrations in New England from observations at a forest flux tower. *J. Geophys. Res.* **104**, 9561–9569.
- Pypker, T. G., Unsworth, M. H., Mix, A. C., Rugh, W., Ocheltree, T. and co-authors. 2007. Using nocturnal cold air drainage flow to monitor ecosystem processes in complex terrain. *Ecol. Appl.* **17**, 702–714.
- Rivier, L., Ciais, P., Hauglustaine, D. A., Bakwin, P., Bousquet, P. and co-authors. 2006. Evaluation of SF₆, C₂Cl₄, and CO to approximate fossil fuel CO₂ in the Northern Hemisphere using a chemistry transport model. *J. Geophys. Res.* **111**, D16311.
- Rödenbeck, C., Houweling, S., Gloor, M. and Heimann, M. 2003. Time-dependent atmospheric CO₂ inversions based on interannually varying tracer transport. *Tellus* **55B**, 488–497.
- Schimel, D. S., House, J. I., Hibbard, K. A., Bousquet, P., Ciais, P. and co-authors. 2001. Recent patterns and mechanisms of carbon exchange by terrestrial ecosystems. *Nature* **414**, 169–172.
- Schimel, D. S., Kittel, T. G. F., Running, S., Monson, R., Turnipseed, A. and co-author. 2002. Carbon sequestration studied in western US mountains. *EOS, Trans. Am. Geophys. Un.* **83**, 445–449.
- Stephens, B. B., Gurney, K. R., Tans, P. P., Sweeney, C., Peters, W. and co-authors. 2007. Weak northern and strong tropical land carbon uptake from vertical profiles of atmospheric CO₂. *Science* **316**, 1732–1735.
- Stuiver, M. and Polach, H. A. 1977. Discussion: reporting of ¹⁴C data. *Radiocarbon* **19**, 355–363.
- Suess, H. E. 1955. Radiocarbon concentration in modern wood. *Science* **122**, 415–417.
- Takahashi, H. A., Konohira, E., Hiyama, T., Minami, M., Nakamura, T. and co-authors. 2002. Diurnal variation of CO₂ concentration, Δ¹⁴C and δ¹³C in an urban forest: estimate of the anthropogenic and biogenic CO₂ contributions. *Tellus* **54B**, 97–109.
- Tans, P. P., de Jong, A. F. M. and Mook, W. G. 1979. Natural atmospheric ¹⁴C variation and the Suess effect. *Nature* **280**, 826–828.
- Turnbull, J. C., Miller, J. B., Lehman, S. J., Tans, P. P., Sparks, R. J. and co-authors. 2006. Comparison of ¹⁴CO₂, CO, and SF₆ as tracers for recently added fossil fuel CO₂ in the atmosphere and implications for biological CO₂ exchange. *Geophys. Res. Lett.* **33**, L01817.
- Turnbull, J. C., Lehman, S. J., Miller, J. B., Sparks, R. J., Southon, J. and co-authors. 2007. A new high precision ¹⁴CO₂ time series for North American continental air. *J. Geophys. Res.* **112**, D11310.
- Wofsy, S. C. and Harriss, R. C. 2002. *The North American Carbon Program (NACP)*, US Global Change Research Program, Washington.
- Wofsy, S. C., Kaplan, W. A. and Harriss, R. C. 1988. Carbon dioxide in the atmosphere over the Amazon Basin. *J. Geophys. Res.* **93**, 1377–1387.